Copy No. 134

CONFIDENTIAL

RM No. A7I06

NACA

RESEARCH MEMORANDUM

AN EXPERIMENTAL INVESTIGATION OF NACA SUBMERGED AIR INLETS ON A 1/5-SCALE MODEL OF A FIGHTER AIRPLANE

By

Donald E. Gault

Ames Aeronautical Laboratory
Moffett Field, Calif.

CLASSIFIED DOCUMENT

This document contains classified information affecting the National Defense of the United States within the meaning of the Espionage Act, USC 50:31 and 32. Its transmission or the revelation of its contents in any manner to an unauthorized person is prohibited by law. Information so classified may be imparted only to persons in the military and naval services of the United States, appropriate civilian officers and employees of the Federal Government who have a legitimate interest therein, and to United States citizens of known loyalty and discretion who of necessity must be informed thereof.

TECHNICAL EDITING WAIVED

NATIONAL ADVISORY COMMITTEE FOR AERONAUTICS

WASHINGTON

December 5, 1947

CONFIDENTIAL

NATIONAL ADVISORY COMMITTEE FOR AERONAUTICS

RESEARCH MEMORANDUM

AN EXPERIMENTAL INVESTIGATION OF NACA SUBMERGED AIR INLETS ON A 1/5-SCALE MODEL OF A FIGHTER AIRPLANE

By Donald E. Gault

SUMMARY

The results of an experimental investigation of an NACA submerged-air-inlet system on a 1/5-scale model of a fighter airplane are presented. Preliminary developmental tests were conducted to select the optimum entrance configuration. Duct-system total-pressure losses and pressure distributions over the lip and ramp of this air intake were obtained. An estimate of the dynamic pressure recovery at the entrance to the jet engine and critical Mach number of the inlet for the fighter airplane is made. It is shown that the inlet location investigated is unsatisfactory.

INTRODUCTION

In conjunction with the general investigation being conducted by the NACA on jet-engine air inlets the development of a submerged-type inlet has been undertaken. The initial experimental work on this inlet can be considered as having consisted of two interdependent phases: (1) basic experimental investigations which were conducted on an isolated inlet mounted in a small wind channel (reference 1), and (2) wind-tunnel studies of complete submerged-inlet systems on scale models of two suitable aircraft. The results from the second phase have been published, in part, as reference 2, but due to the exigencies of wartime wind-tunnel operation, the remaining data, obtained from a 1/5-scale model of a fighter airplane, never progressed beyond preliminary form. Because of the considerable interest now existing in NACA submerged air inlets, the results of the 1/5-scale-model investigation are presented herein.

It will be noted that the plan-form shape of the approach (ramp) to the submerged entrance used for this investigation is not the shape

recommended as optimum in reference 1. The submerged-air-inlet system for the 1/5-scale model of the fighter airplane was designed prior to the completion of the first phase, and the data upon which the recommendations of reference 1 are based were obtained subsequent to the wind-tunnel investigation of this inlet application. The difference in ramp plan forms, which probably decreased the dynamic pressure recovery 2 to 6 percent in the low-inlet-velocity ratio range $(V_e/V_o < 0.7)$ in no way reduces the value of these data as a guide for future submerged-inlet applications.

These tests were requested by the Bureau of Aeronautics, Navy Department, and conducted in the Ames 7- by 10-foot wind tunnel No. 2 during the month of January 1945.

SYMBOLS

The symbols used throughout the report are defined as:

C_L	lift coefficient $\left(\frac{\text{lift}}{\frac{1}{2}\rho V_o^2}\right)$
ΔH	loss in total pressure measured between the free stream and the entrance to the jet engine, pounds per square foot
ΔH_D	loss in total pressure measured between the duct entrance and the entrance to the jet engine, pounds per square foot
ΔH_e	loss in total pressure measured between the free stream and the duct entrance, pounds per square foot
M	Mach number
M_{CR}	critical Mach number
P	pressure coefficient $\left(\frac{p_l - p_o}{q_o}\right)$
p	static pressure, pounds per square foot
q	dynamic pressure $(\frac{1}{2}\rho V^2)$, pounds per square foot
V	velocity, feet per second

V_e/V_o inlet-velocity ratio

α model angle of attack referred to fuselage reference line (wing has 1° incidence), degrees

ρ mass density, slugs per cubic foot

where the subscripts denote conditions for

e duct entrance

o free stream

l local conditions

The expression "percent dynamic pressure recovery" is used to represent the term $100\left[1-(\Delta H/q_o)\right]$. It was assumed to be independent of Mach number in estimating the dynamic pressure recovery for the fighter airplane.

MODEL AND APPARATUS

The 1/5-scale model of the fighter airplane used in the investigation was originally constructed to simulate a jet-boosted aircraft. However, it was assumed for this experimental investigation that the conventional reciprocating engine was removed and that sufficient power for all flight conditions was furnished solely by a Westinghouse 24-C jet engine housed in the fuselage abaft the pilot's enclosure. Full-scale dimensions of the fighter airplane are given in table I, while figure 1 presents a three-view sketch of the airplane. A photograph of the model mounted in the wind tunnel is shown in figure 2. The model, constructed of laminated mahogany on a steel framework, was not provided with a landing gear or empennage. A schematic view of the wind-tunnel test setup is given in figure 3.

For this application, twin NACA submerged entrances, symmetrical about a vertical plane passing through the longitudinal axis of the model, were located along the sides of the fuselage. The lower wall of the ramp was approximately 13 inches (full scale) above the wing chord plane with the lip of the submerged entrance situated immediately above the juncture of the wing leading edge with the fuselage. Each inlet had an entrance area of 0.747 square foot (full scale) which, at 550 miles per hour and an inlet-velocity ratio of 0.60, would furnish at 20,000 feet the required 35.7 pounds per second of air to the Westinghouse 24-C jet engine. The air, after entering the twin submerged inlets, was ducted directly aft until clear of the pilot's enclosure,

and then turned slightly downward and inboard to join in a common channel having an area of 3.142 square feet (full scale) at a distance 3.00 feet (full scale) ahead of the jet-engine compressor. Dimensional characteristics and photographs of the diffuser for the 1/5-scale model are given in figure 4. The deflectors along the ramp walls, which were found to be necessary for maximum ram recovery in reference 1, were molded from modeling clay to simplify making minor modifications in their size and shape while the model was installed in the wind tunnel.

For the investigation reported herein, the air was drawn through the submerged-duct system by a centrifugal pump located outside the wind-tunnel test chamber; power for the pump was furnished by a variable-speed electric motor. Quantity flow through the ducting system was measured by a standard orifice located in the air conduit pipe which connected the model to the pump. Total-pressure losses were determined from an integrating manometer connected to a survey rake consisting of 33 total-head tubes located 6 inches (full scale) upstream of the entrance to the jet-engine compressor. Pressures over the lip and ramp of the submerged entrance were obtained from flush-type orifices located along the center line of the entry and connected to multiple-tube manometers. For several test conditions, total-head survey rakes were placed 5 inches (full scale) downstream of the leading edge of the lip to determine the location and magnitude of the duct-entrance pressure losses.

To determine the efficiency of the internal ducting system, separate bench tests were conducted with the ducts removed from the model and large, bell-shape entrance cones attached to each inlet. Air was drawn through the system by a constant-speed blower and quantity flow varied by a butterfly-type valve located in the blower entrance. Pressure losses and quantity flow were measured with the same rake and orifice previously described and in a similar manner.

PROCEDURE

Prior to installing the model in the wind tunnel the efficiency of the internal ducting system was determined. This information together with entrance losses from a similar submerged inlet served as a guide [1] in the development of the duct-entrance configuration which was thought to be the optimum for the given installation.

Upon selection of the final submerged-inlet configuration, pressure

[1] The method for estimating the maximum dynamic pressure recovery which could be expected in the wind tunnel was identical to that given on page 6 of reference 2.

distributions over the lip and ramp, and duct-system total-pressure losses were measured at constant inlet-velocity ratios throughout a range of angles of attack for flaps retracted and flaps deflected 55°. The effect of airplane yaw on the pressure losses was also determined at several inlet velocities and angles of attack. All pressures were photographically recorded. The critical Mach numbers were estimated by the Kármán-Tsien method outlined in reference 3.

The lift curve and the relationship between the lift coefficient and inlet-velocity ratio for steady, level flight are given in figures 5 and 6, respectively. To estimate the pressure losses and critical Mach number of the lip and ramp throughout the important speed range for the fighter airplane, "matched" lift coefficients and angles of attack corresponding to the inlet-velocity ratios used in this investigation were determined for sea level and 20,000 feet operating conditions. With this information, it was then possible to select the matched flight-condition values of $\Delta H/q_o$ and M_{CR} from plots of the basic wind-tunnel data.

The inlet-velocity ratio was set in the wind tunnel by relating it to the pressure drop across the standard orifice. For inlet-velocity ratios less than 1.60, data were obtained at a tunnel dynamic pressure of 40 pounds per square foot which, based on the mean aerodynamic chord of the model, corresponds to a Reynolds number of approximately 1.4×10^6. Limitations of the centrifugal pump necessitated a reduction in the velocity of the wind tunnel for higher inlet-velocity ratios. Notation is made where the data presented were obtained at lower Reynolds numbers.

RESULTS AND DISCUSSION

Internal Ducting

Bench tests on the internal ducting system showed a total-pressure loss of approximately 18 percent of the duct-entrance dynamic pressure. (See fig. 7.) Velocity distributions measured at the plane of the survey rake (fig. 8) and a tuft study disclosed no regions of turbulent or separated flow, and it is probable that guide vanes would not have decreased this pressure loss appreciably.

Preliminary Studies

The initial wind-tunnel tests showed greater over-all total-pressure losses than had been expected for this installation. As a result, until the causes for the discrepancy were discovered and the condition remedied, the original test program to determine the characteristics of the inlet through the flight range was temporarily postponed.

When the efficiency of the internal ducting system was considered, it appeared that some unknown flow condition was causing entrance losses far in excess of those ordinarily obtainable with a submerged inlet. Readings from a total-pressure survey rake (fig. 9) installed in the duct entrance verified the abnormal nature of the losses and revealed that the region of low energy air was located in the corners of the inlets nearest the wing. Further investigation using tufts disclosed that upwash from the adjacent wing was effectively adding a component of flow perpendicular to the center line of the ramp and distorting the normal streamline pattern over the submerged entrance. This distortion was noticeable along only the lower side (i.e., the side nearest the wing) of the ramp and resulted in separated flow which passed downstream and into the inlet. The use of extended deflectors (reference 1) reduced the entrance losses markedly (fig. 9) with a consequent gain in the dynamic pressure recovery over that obtained with the plain duct (fig. 10)[2].

The use of deflectors for this investigation should not be considered solely as having been a means of preventing the boundary-layer air from entering the inlet as explained in reference 1. Tuft studies indicated that the lower deflectors prevented the oblique flow over the lower corner of the entrance and, hence, eliminated the pressure losses resulting from separation. Unfortunately, the height of the deflectors required to accomplish this was more than twice that which was recommended in reference 1. A more forward inlet position, free from the influence of the wing-flow field, would have undoubtedly permitted the use of smaller deflectors similar to those investigated in reference 2. Not only would the boundary-layer thickness have decreased, but the necessity for large lower deflectors to prevent separation would have been eliminated. The upper and lower deflectors for this investigation were made identical for reasons of symmetry only, although smaller deflectors along the upper edge of the ramp would have been equally effective. Ordinates and details of the final submerged-inlet configuration are shown in figure 11.

Pressure Losses

The total pressure losses at the simulated entrance to the jet engine and pressure distributions over the lip and ramp were obtained upon selection of the final inlet configuration. Table II presents the total pressure losses as a fraction of the free-stream dynamic pressure $\Delta H/q_0$ for constant inlet-velocity ratios throughout a range of angles of attack.

[2] These data were obtained with the pressure survey rakes installed in the duct entrance and are shown for comparative purposes only.

Figure 12 shows the variation at sea level and 20,000 feet of the duct-system total-pressure loss with airplane lift coefficient for the fighter airplane as determined from this investigation. The percent dynamic-pressure recovery as a function of airplane velocity is presented in figure 13 for the same conditions. It will be seen that the maximum dynamic-pressure recovery obtained was 83 percent for conditions simulating 550 miles per hour at sea level and 20,000 feet. Decreasing the flight speed to 350 miles per hour corresponded to only a 6-percent decrease in the recovery, but thereafter it falls off more rapidly. For the take-off static-thrust condition when the free-stream velocity and dynamic pressure are zero ($V_e/V_o = \infty$) approximately 33 percent of the duct-entrance dynamic pressure was lost.

The effect of yaw on the ram recovery is presented in figure 14. No sudden discontinuities in the recovery for increasing angles of yaw are indicated.

Again it should be noted that the plan-form shape of the ramp used for this investigation is not the optimum for maximum dynamic-pressure recovery. The recommendations given in reference 1 for the optimum ramp shape are based on data obtained subsequent to the wind-tunnel tests reported herein. As mentioned before, this difference in ramp shapes amounts to a decrease in the ram recovery of approximately 2 to 6 percent, depending on the inlet-velocity ratio.

Pressure Distribution

The pressure distributions over the lip and ramp are given in terms of the pressure coefficient P in tables III and IV, respectively. Inspection of these data will show a considerable variation in the distributions with angle of attack. Pressures over the basic fuselage contour along the center line of the entry for several angles of attack (fig. 15) demonstrate that this variation is due primarily to the location of the inlet in the flow field of the wing. This effect on the critical Mach number M_{CR} of the lip[3] is clearly seen in figure 16.

The variation with true airspeed of the submerged-inlet critical Mach number is given in figure 17 for the fighter airplane as determined from these data.

Although the decrease in M_{CR} from sea level to 20,000 feet operating conditions is comparatively small, it is directly attributable to the effect the change in angle of attack incurs in the velocities

[3]The critical Mach number of the ramp is not presented since, for all conditions investigated, it was higher than that for the lip.

superimposed over the duct entrance. For an airplane having a higher wing loading and operating at greater altitudes, the resulting increased angle of attack for a given flight speed would have a more pronounced effect in reducing M_{CR}. The pressure-distribution data indicate that the critical Mach number could have been increased if the entrance had been located 20 to 30 inches (full scale) farther forward. The assumption is made, however, that in moving the inlet forward the ramp would not be placed in the field of a strong pressure gradient as existed behind the cowl leading edge for this investigation (fig. 15). The pressure peak over the cowl, caused by zero inflow through the cowl entrance, cannot be considered as representative for a more streamlined nose shape which would be incorporated on a completely jet-propelled aircraft.

It is emphasized that selection of the final duct-entrance configuration was based solely on considerations of maximum dynamic-pressure recovery and critical Mach number of the lip and ramp. No drag evaluations or deflector critical Mach number studies were made.

Duct-flow Instability

Throughout this investigation an unstable duct flow occurred at inlet-velocity ratios less than approximately 0.45. This instability originated with a decrease in quantity flow through one inlet and an increase in quantity flow for the opposite inlet with no appreciable change in the total quantity flow through the internal ducting system. The divergence from equal flows through the twin entries continued until zero inflow resulted in the one duct, at which time a complete reversal took place and the flows through the two entries equalized. The disturbance was cyclic and, once started, continued until the total quantity flow through the system was increased sufficiently to raise the average inlet-velocity ratio above approximately 0.45. The decrease in flow from the stable condition always occurred in the same inlet. No pressure losses or pressure-distribution measurements could be measured due to the rapid fluctuations of the liquid in the manometer tubes.

It cannot be assumed, however, that the instability would occur at these same values of inlet-velocity ratio on the fighter airplane. The unstable regime is a function of the losses in the internal ducting system, and differences in fabrication, even between individual production-line aircraft, would consequently cause small variations in the value of the inlet-velocity ratio at which instability commenced. Mechanical methods of eliminating this condition are discussed in reference 2.

CONCLUSIONS

The results of a wind-tunnel investigation of an NACA submerged-air-inlet system on a 1/5-scale model of a fighter airplane indicate that:

1. The location of the duct entrance was unsatisfactory due to its position in reference to the wing.

2. A submerged inlet should not be placed on a surface where flow oblique to the center line of the ramp will occur.

3. A submerged inlet should not be placed on a surface where high incremental velocities will be superimposed over the ramp and lip.

Ames Aeronautical Laboratory,
National Advisory Committee for Aeronautics,
Moffett Field, Calif.

REFERENCES

1. Frick, Charles W., Davis, Wallace F., Randall, Lauros M., and Mossman, Emmet A.: An Experimental Investigation of NACA Submerged-Duct Entrances. NACA ACR No. 5120, 1945.

2. Mossman, Emmet A., and Gault, Donald E.: Development of NACA Submerged Inlets and a Comparison with Wing Leading-Edge Inlets for a 1/4-Scale Model of a Fighter Airplane. NACA CRM No. A7A31, 1947.

3. von Kármán, Th.: Compressibility Effects in Aerodynamics. Jour. Aero. Sci., vol. 8, no. 9, July 1941, pp. 337-356.

TABLE I
DIMENSIONS OF THE FIGHTER AIRPLANE

Airplane, general	
Over-all span	40 ft, 0 in.
Over-all length	30 ft, 1/4 in.
Over-all height (at rest)	13 ft, 8 in.
Weight	8400 lb
Wing	
Airfoil section	
Root	NACA 65_2-117(a=1.0)
Tip	NACA 65_2-115(a=0.5)
Total area	275 sq ft
Chord	
Root	112 in.
Tip	56 in.
Mean aerodynamic chord	87.55 in.
Dihedral angle of chord plane	
Center panel	0°
Outer panels	7-1/2°
Incidence (with respect to fuselage reference line)	1°
Flaps	
Type	Douglas retractable deflecting slot
Span	
Inner	4 ft, 6-1/2 in.
Outer	4 ft, 8-1/2 in.
Chord	0.25 wing chord
Total area	30.25 sq ft
Engine	Westinghouse 24-C
Rating	3000 lb static thrust at sea level (12,000 rpm)

NATIONAL ADVISORY COMMITTEE FOR AERONAUTICS.

TABLE II

DUCT-SYSTEM TOTAL-PRESSURE LOSSES FOR THE 1/5-SCALE MODEL OF THE FIGHTER AIRPLANE EQUIPPED WITH NACA SUBMERGED AIR INLETS

Flaps Retracted										
Total Pressure Loss, $\Delta H/q_o$										
V_e/V_o \ α	-3.76	-2.68	-1.60	-0.49	0.61	1.71	2.80	3.90	6.07	9.31
0.5	0.157	0.168	0.172	0.193	0.209	- -	- -	- -	- -	- -
0.6	.171	.163	.163	.173	.178	.183	- -	- -	- -	- -
0.8	.179	.178	.178	.188	.194	.188	.189	- -	- -	- -
1.0	- -	.215	.219	.230	.231	.240	.236	.236	- -	- -
1.2	- -	- -	.271	.280	.292	.301	.293	.290	.285	- -
1.4	- -	- -	- -	.377	.372	.372	.370	.374	.393	.374
1.6	- -	- -	- -	- -	.480	.486	.488	.488	.498	.494
2.0	- -	- -	- -	- -	- -	.754	.752	.760	.744	.749
2.5	- -	- -	- -	- -	- -	- -	1.223	1.203	1.179	1.195

Flaps Deflected 55°								
V_e/V_o \ α	-4.60	-2.55	-0.33	1.90	4.10	6.23	8.44	10.65
2.5	1.161	1.173	1.195	1.236	1.257	1.226	1.195	1.161
3.0	1.663	1.696	1.794	1.878	1.857	1.917	1.857	1.758
3.5	2.049	2.088	2.148	2.290	2.358	2.358	2.300	2.279
4.0	2.660	2.773	2.870	2.973	3.074	2.998	2.915	2.915

NATIONAL ADVISORY COMMITTEE FOR AERONAUTICS

TABLE III

PRESSURE DISTRIBUTION OVER THE LIP OF THE NACA SUBMERGED AIR INLET ON THE 1/5-SCALE MODEL OF THE FIGHTER AIRPLANE

V_e/V_o = 0.60															
Pressure Coefficient, P															
Sta. / α	Inside					Lip L.E.	Outside								
	23.80	22.30	22.05	21.93	21.83	21.80	21.83	21.93	22.05	22.30	22.80	23.30	24.30	25.30	26.30
-2.68	0.534	0.489	0.692	0.682	0.667	-0.127	-0.494	-0.433	-0.473	-0.463	-0.382	-0.371	-0.321	-0.300	-0.204
-1.60	.519	.483	.692	.687	.667	-.198	-.595	-.509	-.550	-.545	-.458	-.443	-.392	-.361	-.254
-.49	.494	.453	.682	.677	.662	-.193	-.616	-.539	-.590	-.595	-.514	-.499	-.453	-.412	-.300
.61	.468	.422	.687	.682	.667	-.178	-.646	-.575	-.636	-.656	-.590	-.575	-.524	-.489	-.356
2.80	.463	.407	.687	.677	.667	-.188	-.733	-.667	-.753	-.799	-.738	-.728	-.667	-.626	-.483
6.07	.473	.392	.692	.687	.677	-.142	-.799	-.789	-.911	-.967	-.962	-.941	-.850	-.814	-.646
V_e/V_o = 0.80															
-2.68	.263	.182	.076	.197	.750	.354	-.111	-.187	-.273	-.354	-.339	-.349	-.324	-.319	-.228
-1.60	.273	.197	.091	.223	.770	.309	-.177	-.238	-.329	-.410	-.390	-.395	-.375	-.365	-.268
-.49	.253	.167	.061	.187	.744	.304	-.213	-.273	-.375	-.466	-.450	-.466	-.435	-.425	-.304
.61	.233	.137	.010	.152	.719	.304	-.243	-.314	-.425	-.532	-.526	-.546	-.516	-.496	-.365
2.80	.244	.112	-.041	.097	.672	.326	-.285	-.372	-.509	-.652	-.662	-.687	-.656	-.651	-.488
6.07	.244	.041	-.163	-.076	.458	.438	-.265	-.417	-.600	-.819	-.855	-.886	-.840	-.794	-.636

NATIONAL ADVISORY
COMMITTEE FOR AERONAUTICS

TABLE III.- Concluded

V_e/V_o = 1.00															
Pressure Coefficient, P															
Sta. / α	Inside					Lip L.E.	Outside								
	22.80	22.30	22.05	21.93	21.83	21.80	21.83	21.93	22.05	22.30	22.80	23.30	24.30	25.30	26.30
-1.60	-.061	-.260	-.504	-.402	.254	.712	.214	.020	-.112	-.280	-.326	-.361	-.356	-.356	-.249
-.49	-.092	-.300	-.554	-.448	.209	.712	.178	.010	-1.53	-.336	-.387	-.428	-.428	-.428	-.305
.61	-.102	-.346	-.610	-.508	.142	.728	.163	0	-.188	-.392	-.458	-.504	-.499	-.489	-.356
2.80	-.107	-.361	-.672	-.580	-.494	.738	.132	.006	-.265	-.494	-.580	-.631	-.631	-.620	-.468
6.07	-.102	-.346	-.830	-.794	-.305	.814	.163	-.102	-.326	-.636	-.753	-.814	-.804	-.774	-.616
9.31	-.117	-.382	-1.106	-1.170	-.820	.911	.265	-.102	-.377	-.774	-.931	-1.003	-.977	-.942	-.768
	V_e/V_o = 1.20														
-1.60	-.504	-.758	-1.252	-1.266	-.575	.942	.529	.260	.092	-.142	-.244	-.305	-.321	-.326	-.234
-.49	-.519	-.763	-1.293	-1.293	-.626	.946	.488	.219	.046	-.203	-.321	-.387	-.402	-.402	-.295
.61	-.530	-.774	-1.344	-1.344	-.697	.936	.468	.194	.005	-.260	-.382	-.452	-.473	-.463	-.351
2.80	-.560	-.799	-1.481	-1.491	-.931	.952	.458	.173	-.041	-.346	-.489	-.524	-.540	-.540	-.448
6.07	-.540	-.784	-1.700	-1.761	-1.400	.992	.489	.153	-.102	-.489	-.682	-.778	-.789	-.768	-.560
9.31	-.644	-.916	-2.118	-2.224	-2.127	1.000	.575	.158	-.143	-.631	-.866	-.972	-.988	-.962	-.774

TABLE IV

PRESSURE DISTRIBUTION OVER THE RAMP OF THE NACA SUBMERGED AIR INLET ON THE 1/5-SCALE MODEL OF THE FIGHTER AIRPLANE

V_e/V_o = 0.60												
Pressure Coefficient, P												
α \ sta.	11.20	12.25	13.25	14.25	15.25	16.25	17.25	18.25	19.25	20.25	21.25	22.25
-2.68	-0.311	-0.188	-0.163	-0.137	-0.112	-0.092	-0.015	0.087	0.239	0.417	0.545	0.575
-1.60	-.311	-.199	-.173	-.148	-.132	-.112	-.046	.056	.219	.402	.530	.570
- .49	-.305	-.204	-.178	-.158	-.148	-.132	-.071	-.031	.193	.377	.499	.540
.61	-.326	-.224	-.209	-.188	-.178	-.173	-.112	-.010	.158	.351	.473	.514
2.80	-.354	-.266	-.251	.240	-.240	-.240	-.184	-.082	.102	.322	.445	.512
6.07	-.413	-.327	-.322	-.327	-.338	-.353	-.292	-.197	-.005	.272	.418	.489
V_e/V_o = 0.80												
-2.68	-.309	-.192	-.172	-.147	-.137	-.116	-.076	.046	.167	.314	.440	.400
-1.60	-.309	-.203	-.172	-.157	-.142	-.127	-.081	.020	.192	.294	.430	.395
- .49	-.309	-.213	-.192	-.167	-.162	-.152	-.111	-.010	.116	.273	.405	.380
.61	-.314	-.223	-.203	-.192	-.187	-.187	-.152	-.056	.081	.243	.390	.370
2.80	-.346	-.265	-.254	-.244	-.254	-.260	-.219	-.122	.010	.194	.366	.366
6.07	-.412	-.326	-.331	-.331	-.351	-.372	-.331	-.244	-.107	.107	.321	.351

TABLE IV.- Concluded

$[V_e/V_o = 1.00]$

Pressure Coefficient, P												
Sta. / α	11.20	12.25	13.25	14.25	15.25	16.25	17.25	18.25	19.25	20.25	21.25	22.25
-1.60	-.311	-.205	-.175	-.160	-.150	-.150	-.100	-.030	.080	.190	.271	.140
- .49	-.319	-.218	-.198	-.187	-.182	-.182	-.142	-.071	.046	.162	.243	.111
.61	-.326	-.234	-.214	-.209	-.209	-.214	-.183	-.117	.005	.127	.224	.102
2.80	-.355	-.268	-.258	-.258	-.263	.279	.243	-.177	-.056	.081	.203	.101
6.07	-.415	-.329	-.334	-.339	-.355	-.390	-.349	.294	-.167	.015	.157	.086
9.31	-.499	-.422	-.427	-.452	-.494	-.540	-.499	-.442	-.324	-.144	.098	.067
$V_e/V_o = 1.20$												
-1.60	-.314	-.203	-.182	-.167	-.152	-.162	-.127	-.071	.020	.086	.081	-.187
- .49	-.321	-.224	-.204	-.193	-.193	-.199	-.173	-.117	-.020	.051	.061	-.199
.61	-.327	-.237	-.222	-.212	-.217	-.232	-.207	-.146	-.055	.025	.055	-.207
2.80	-.354	-.268	-.258	-.258	-.268	-.294	-.268	-.218	-.117	-.030	.005	-.233
6.07	-.417	-.314	-.346	-.356	-.382	-.412	-.392	-.341	-.249	-.132	-.041	-.234
9.31	-.517	-.434	-.439	-.470	-.517	-.574	-.548	-.502	-.414	-.274	-.114	-.258

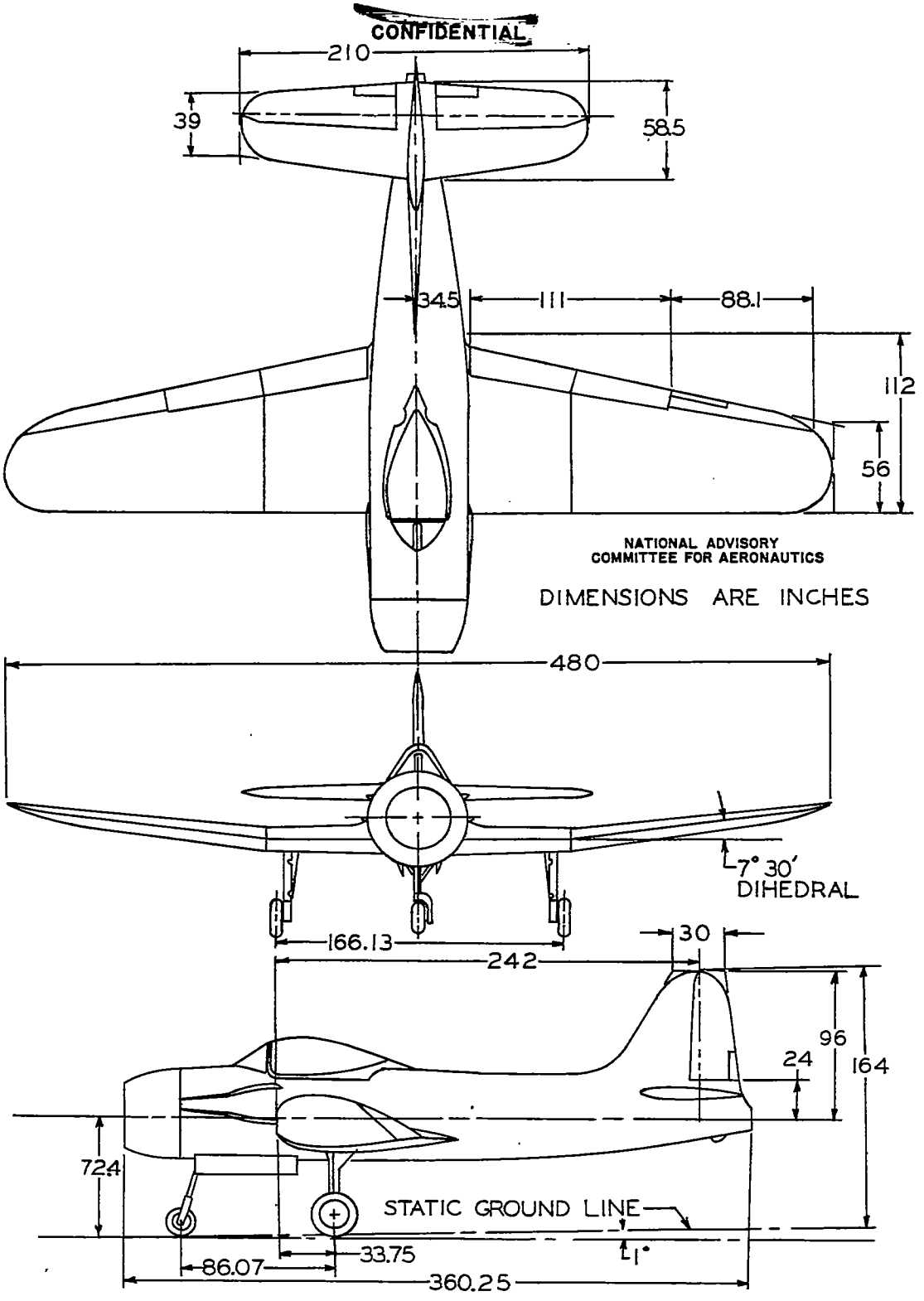

FIGURE 1.-GENERAL ARRANGEMENT OF THE FIGHTER AIRPLANE EQUIPPED WITH NACA SUBMERGED AIR INLETS.

CONFIDENTIAL

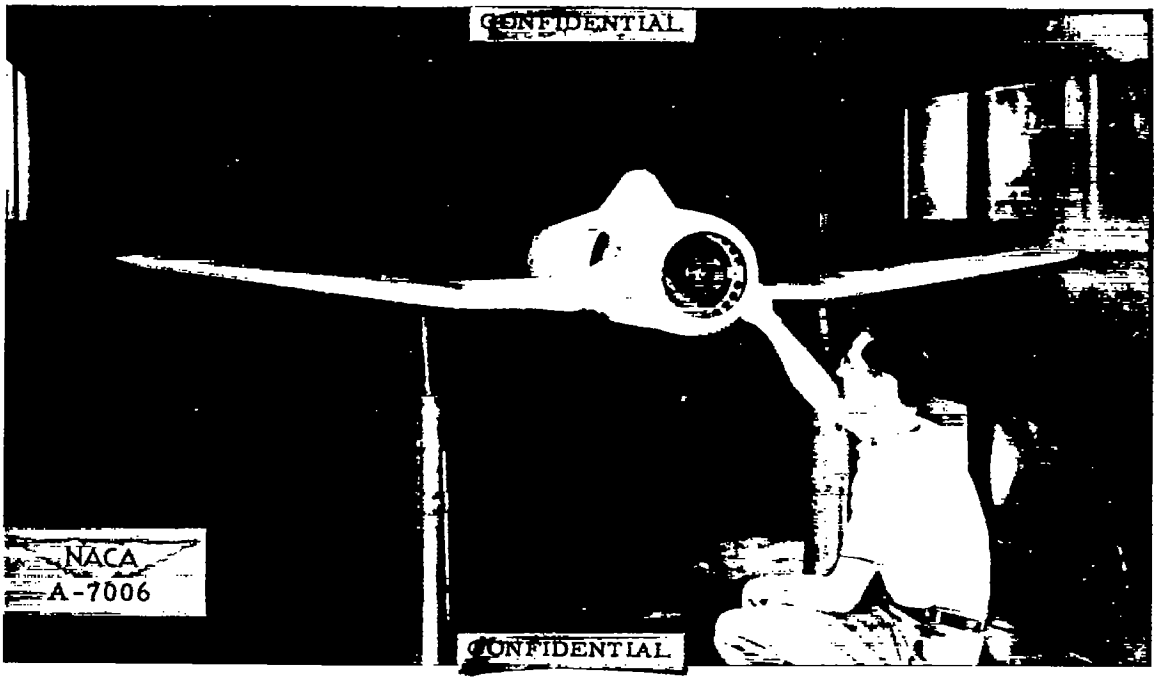

Figure 2.- The 1/5-scale model of the fighter airplane equipped with NACA submerged air inlets installed in the Ames 7- by 10-foot wind-tunnel No. 2.

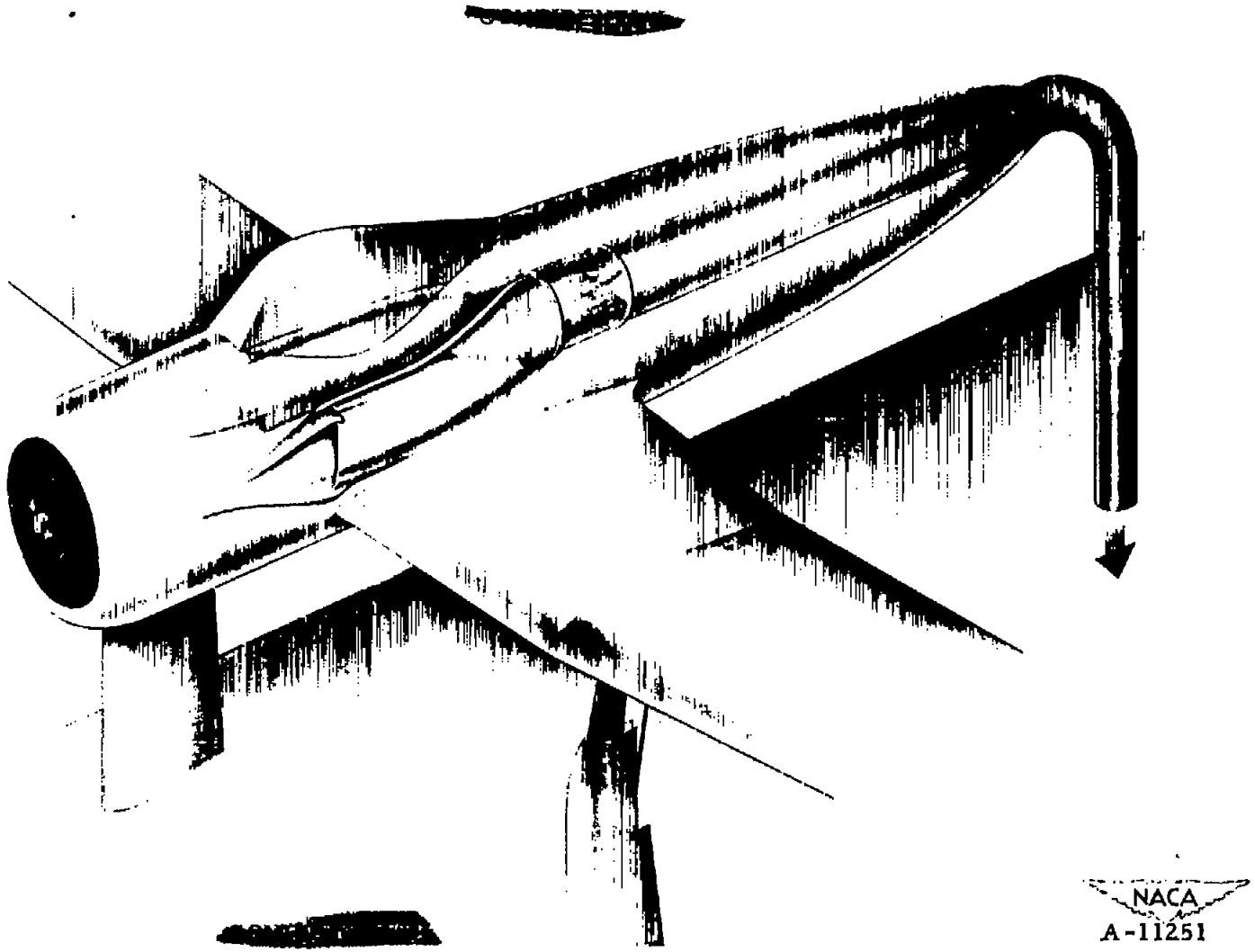

Figure 3.— Schematic view of the wind-tunnel test setup for the 1/5-scale model of the fighter airplane equipped with NACA submerged air inlets.

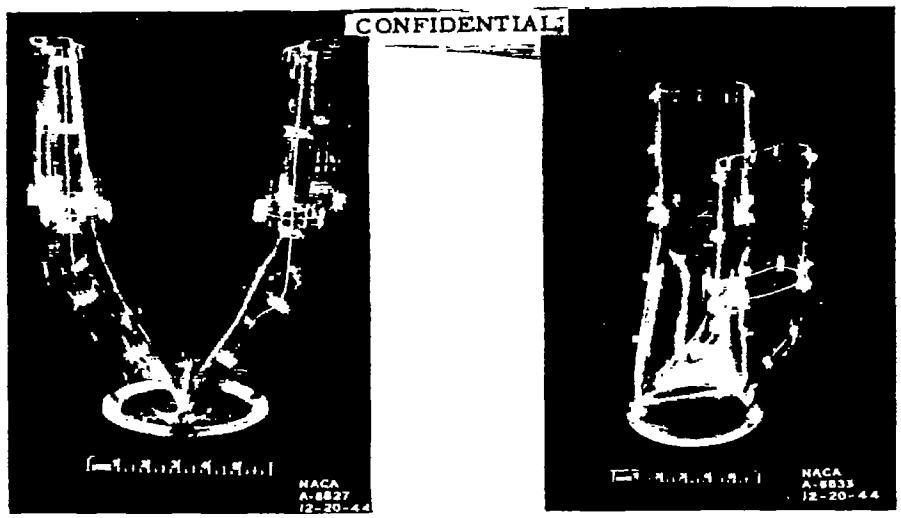

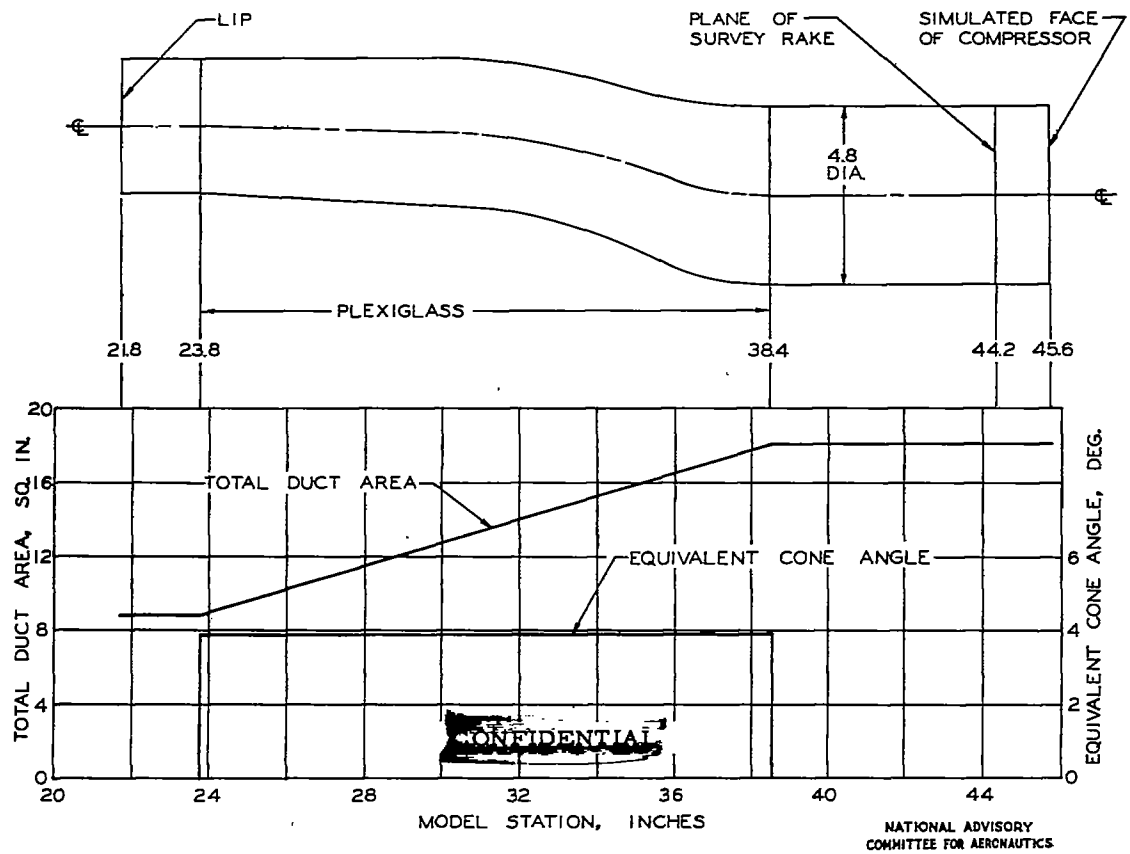

Figure 4.— Dimensional Characteristics of the internal-ducting system to the stimulated face of the jet-engine compressor for the 1/5-scale model of the fighter airplane equipped with submerged ducts.

CONFIDENTIAL

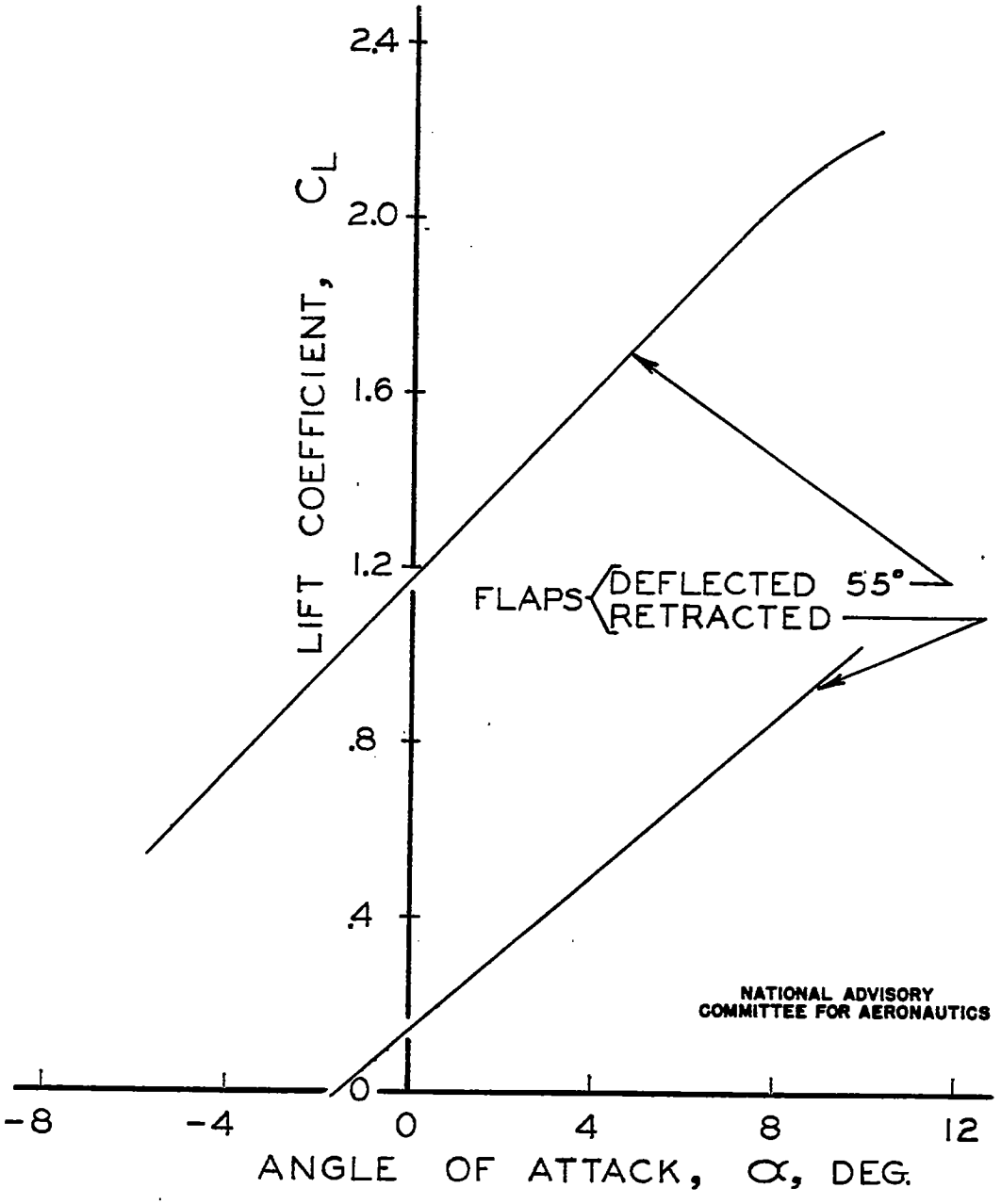

FIGURE 5.–VARIATION OF THE LIFT COEFFICIENT WITH ANGLE OF ATTACK FOR THE 1/5-SCALE MODEL OF THE FIGHTER AIRPLANE. RN = 1.41×10^6

CONFIDENTIAL

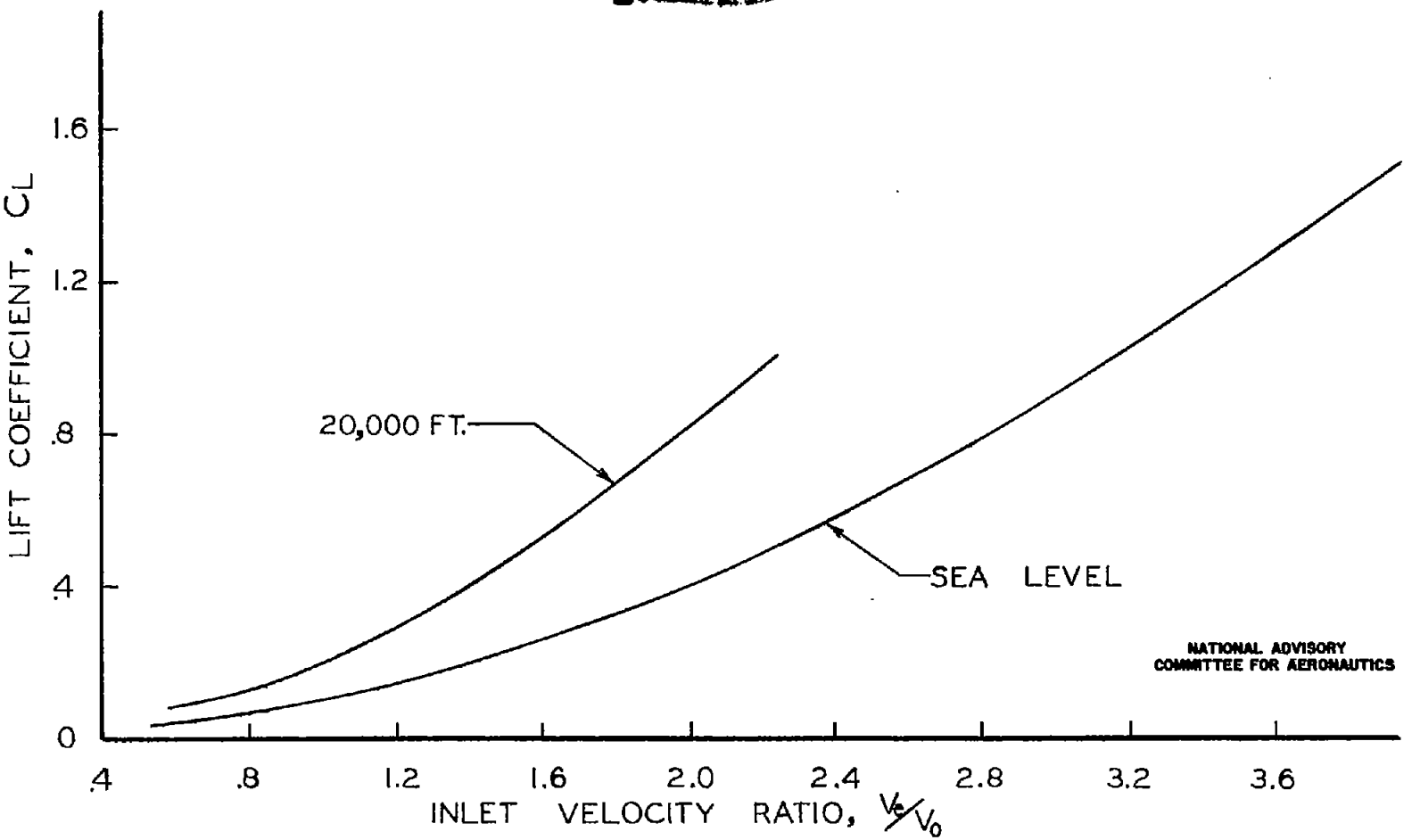

FIGURE 6.-VARIATION OF INLET-VELOCITY RATIO WITH LIFT COEFFICIENT FOR THE FIGHTER AIRPLANE EQUIPPED WITH A WESTINGHOUSE 24C JET ENGINE OPERATING AT MILITARY RATED POWER. DUCT-ENTRANCE AREA = 1.494 SQ. FT.

CONFIDENTIAL

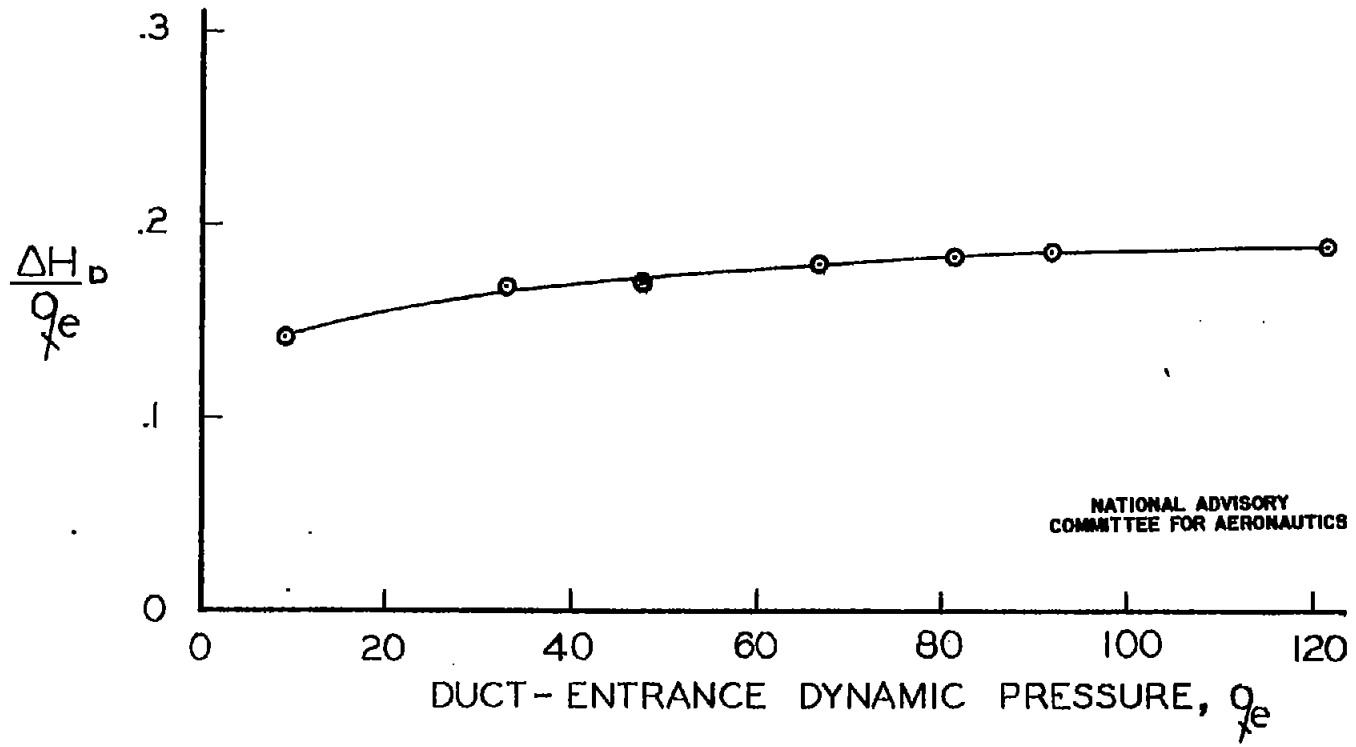

FIGURE 7.-VARIATION OF THE INTERNAL-DUCTING LOSSES WITH DUCT-ENTRANCE DYNAMIC PRESSURE FOR THE 1/5-SCALE MODEL OF THE FIGHTER AIRPLANE EQUIPPED WITH NACA SUBMERGED DUCT ENTRIES.

CONFIDENTIAL

CONFIDENTIAL

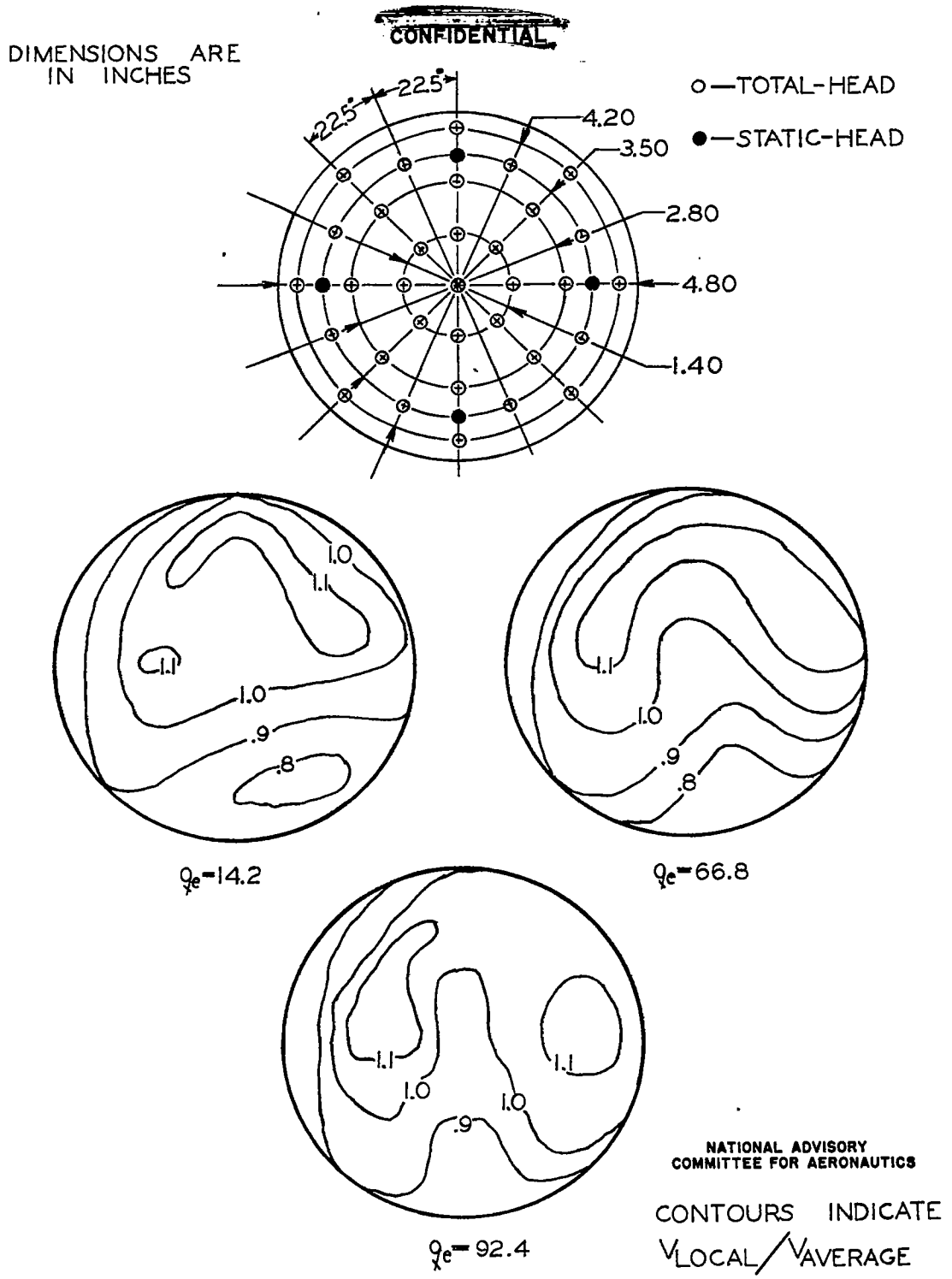

FIGURE 8.-DETAILS OF PRESSURE SURVEY RAKE AND VELOCITY DISTRIBUTIONS AT THE ENTRANCE TO THE JET ENGINE FOR THE 1/5-SCALE MODEL OF FIGHTER AIRPLANE.

CONFIDENTIAL

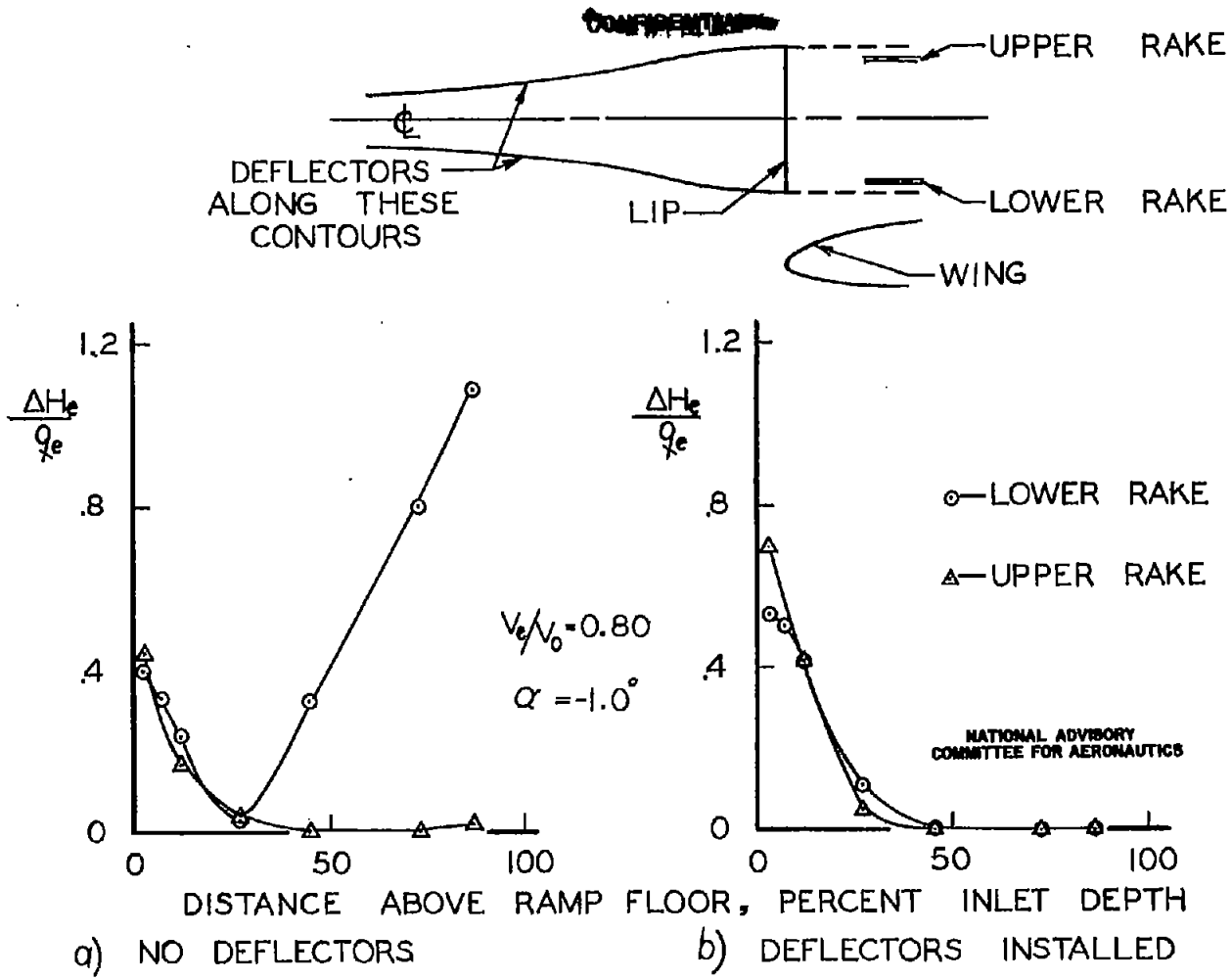

FIGURE 9.-COMPARISON OF THE SUBMERGED INLET ENTRANCE LOSSES WITH AND WITHOUT DEFLECTORS FOR THE 1/5-SCALE MODEL OF THE FIGHTER AIRPLANE. $RN = 1.41 \times 10^6$

CONFIDENTIAL

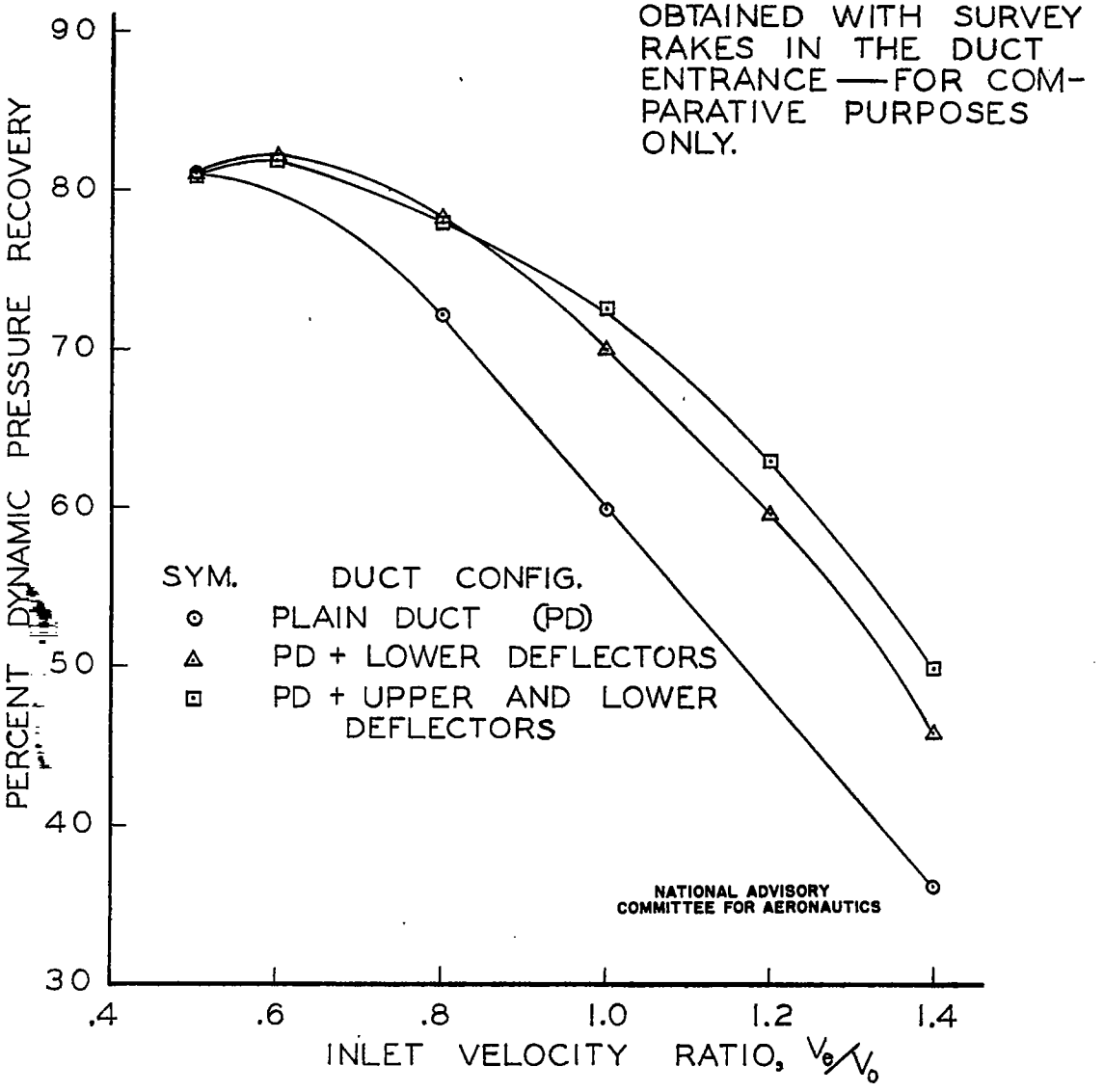

FIGURE 10.-EFFECT OF DEFLECTORS ON THE VARIATION OF THE DYNAMIC-PRESSURE RECOVERY WITH INLET-VELOCITY RATIO FOR THE 1/5-SCALE MODEL OF THE FIGHTER AIRPLANE. $\alpha = 0°$, $RN = 1.41 \times 10^6$

CONFIDENTIAL

LIP

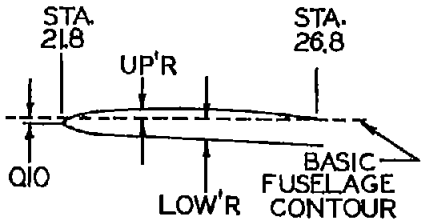

STA.	UP'R	LOW'R
21.80	——	0.100
22.05	0.087	.290
22.30	.147	.330
22.55	.172	.360
22.80	.189	.375
23.30	.203	2.9° SLOPE
23.80	.196	
24.30	.179	
24.80	.152	
25.30	.116	
25.80	.090	
26.30	.035	
26.80	0	

L.E. RAD.=0.100

RAMP

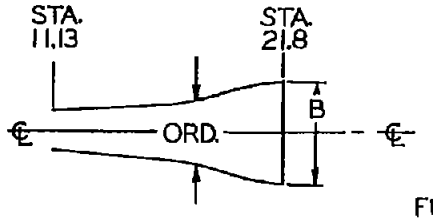

STA.	ORD.
11.13	1.28
12.20	1.38
13.26	1.48
14.33	1.58
15.40	1.70
16.47	1.98
17.53	2.48
18.60	3.26
19.67	3.90
20.73	4.22
21.80	4.25

B=4.28=CHORD OF 34.5° ARC OF 7.22 RADIUS (FUSELAGE CONTOUR AT STA. 21.80)

DEFLECTORS

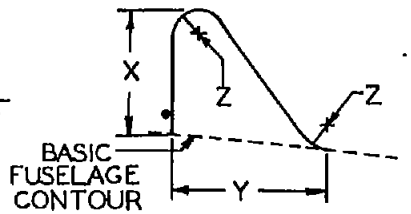

STA.	X	STA.	X
23.30	0	20.05	0.94
23.05	0.20	19.80	.90
22.80	.36	19.30	.78
22.55	.51	18.80	.66
22.30	.64	18.30	.54
22.05	.74	17.80	.49
21.80	.82	17.30	STRAIGHT LINE
21.55	.88		
21.30	.92		
21.05	.95		
20.80	.97		
20.55	.97		
20.30	.96	11.13	0

Y = 1.44X Z = 0.21X

NATIONAL ADVISORY COMMITTEE FOR AERONAUTICS

ALL ORDINATES AND STATIONS ARE IN INCHES

FIGURE 11.-LIP, RAMP, AND DEFLECTOR ORDINATES FOR THE FINAL CONFIGURATION OF THE NACA SUBMERGED AIR INLETS INVESTIGATED ON THE 1/5-SCALE MODEL OF THE FIGHTER AIRPLANE.

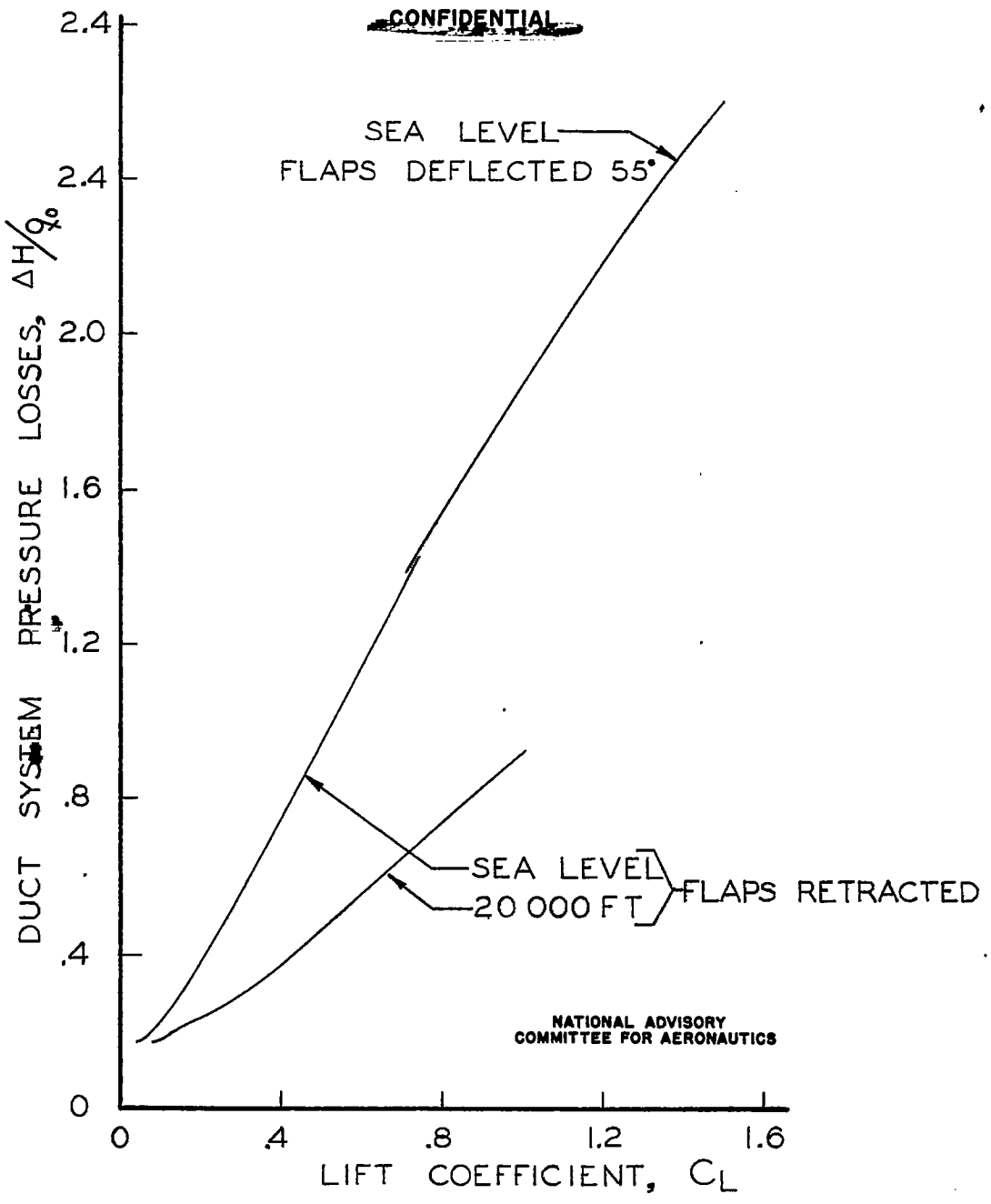

FIGURE 12.-VARIATION OF THE DUCT-SYSTEM PRESSURE LOSSES WITH LIFT COEFFICIENT FOR THE 1/5-SCALE MODEL OF THE FIGHTER AIRPLANE. "MATCHED" FLIGHT CONDITIONS AT SEA LEVEL AND 20,000 FT.

CONFIDENTIAL

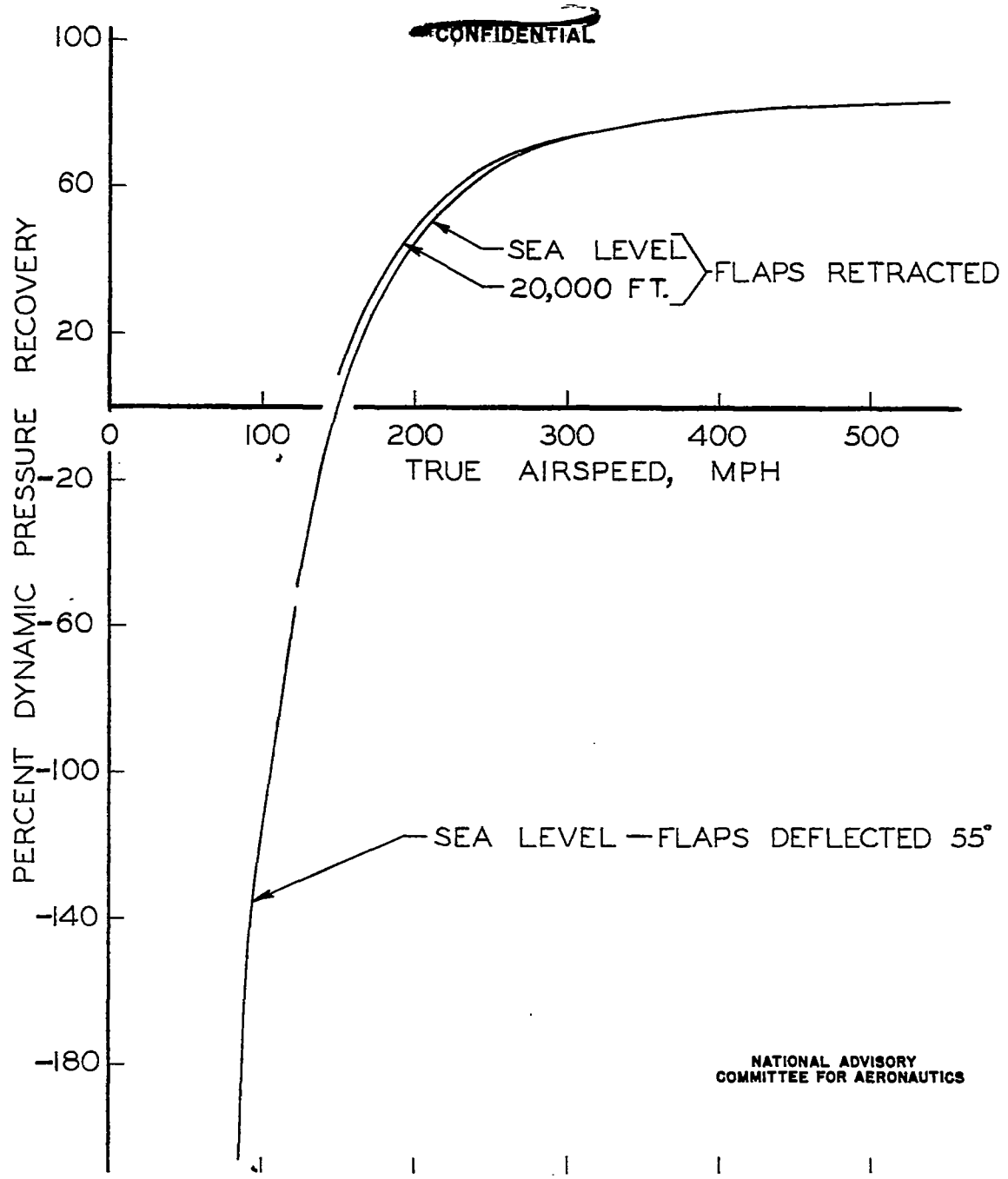

FIGURE 13.-VARIATION OF THE DYNAMIC PRESSURE RECOVERY WITH TRUE AIRSPEED ESTIMATED FOR THE FIGHTER AIRPLANE. "MATCHED" FLIGHT CONDITIONS AT SEA LEVEL AND 20,000 FT.

CONFIDENTIAL

CONFIDENTIAL

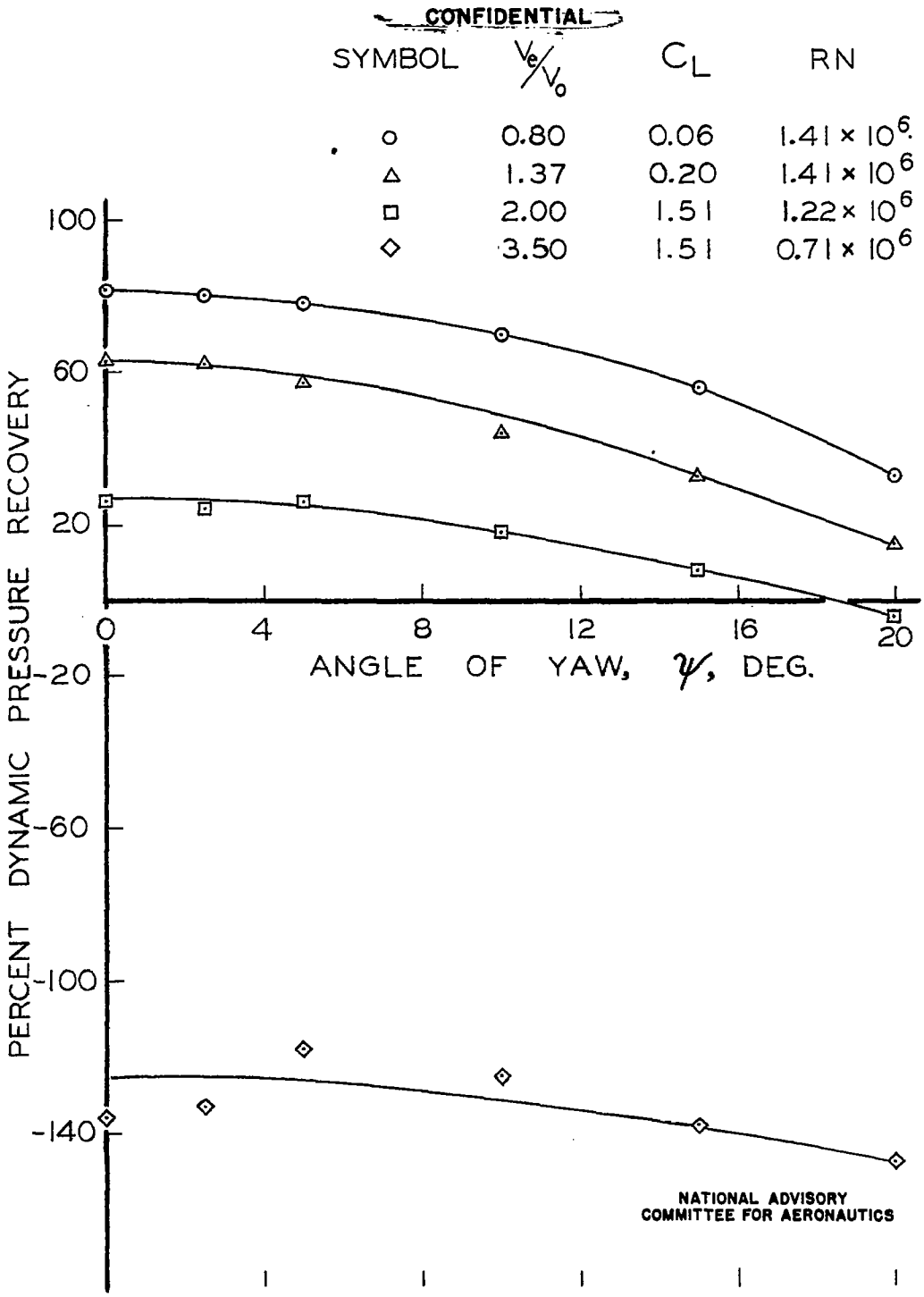

FIGURE 14.-VARIATION OF THE DYNAMIC-PRESSURE RECOVERY WITH ANGLE OF YAW FOR THE 1/5-SCALE MODEL OF THE FIGHTER AIRPLANE.

CONFIDENTIAL

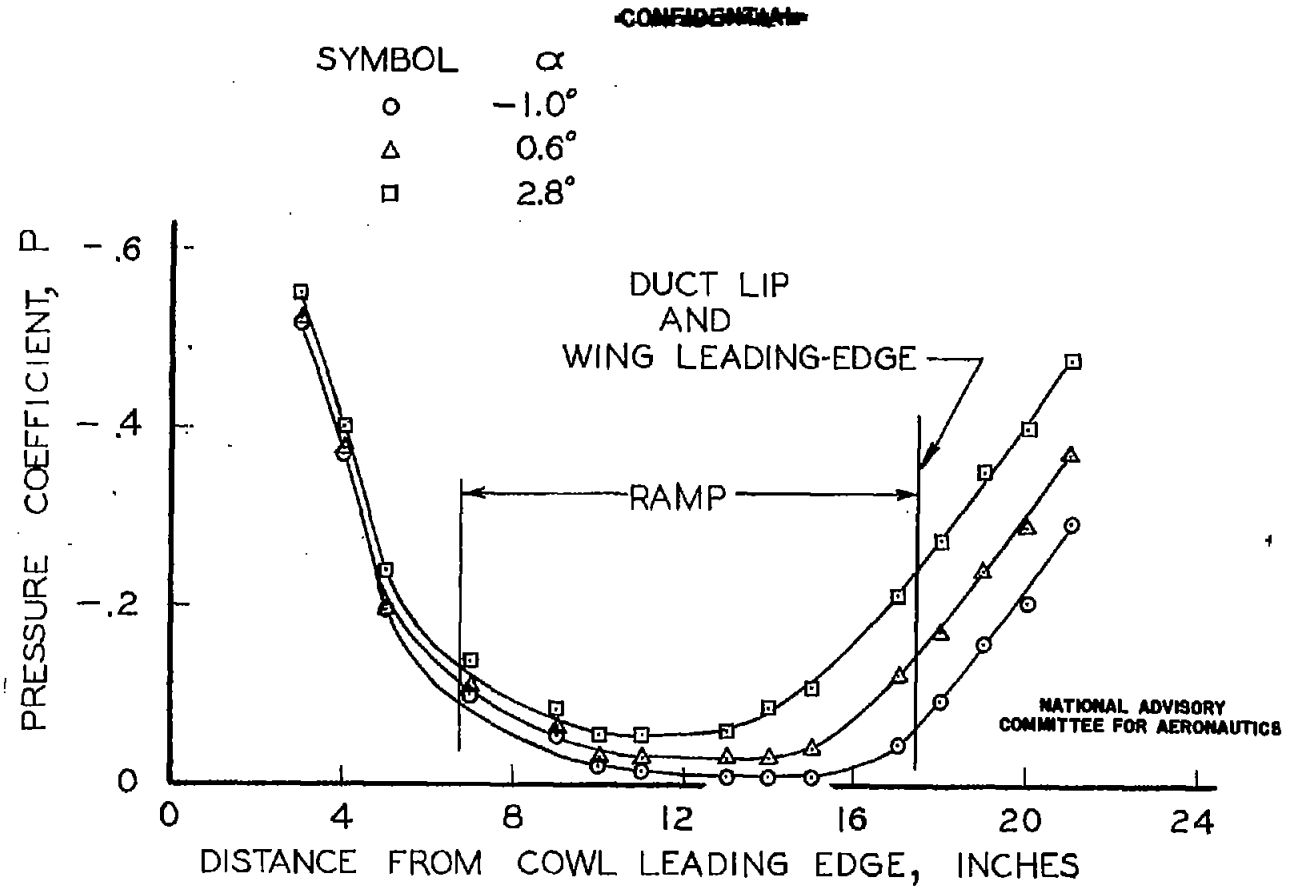

FIGURE 15.—PRESSURE DISTRIBUTION OF THE BASIC FUSELAGE CONTOUR ALONG THE ℄ OF THE NACA SUBMERGED DUCT ENTRY. 1/5-SCALE MODEL OF THE FIGHTER AIRPLANE. RN = 1.41×10^6

CONFIDENTIAL

CONFIDENTIAL

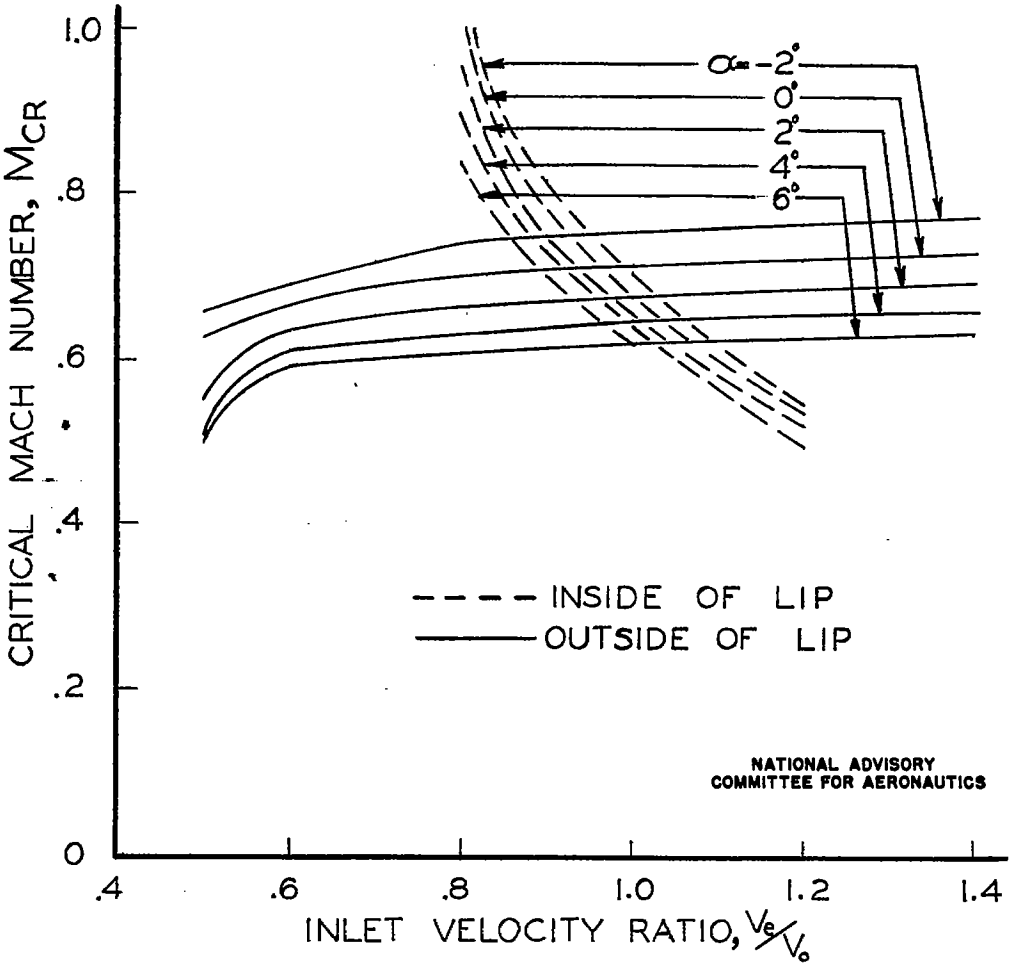

FIGURE 16.-EFFECT OF ANGLE OF ATTACK ON THE VARIATION OF THE LIP ESTIMATED CRITICAL MACH NUMBER WITH INLET-VELOCITY RATIO FOR THE 1/5-SCALE MODEL OF THE FIGHTER AIRPLANE.

CONFIDENTIAL

CONFIDENTIAL

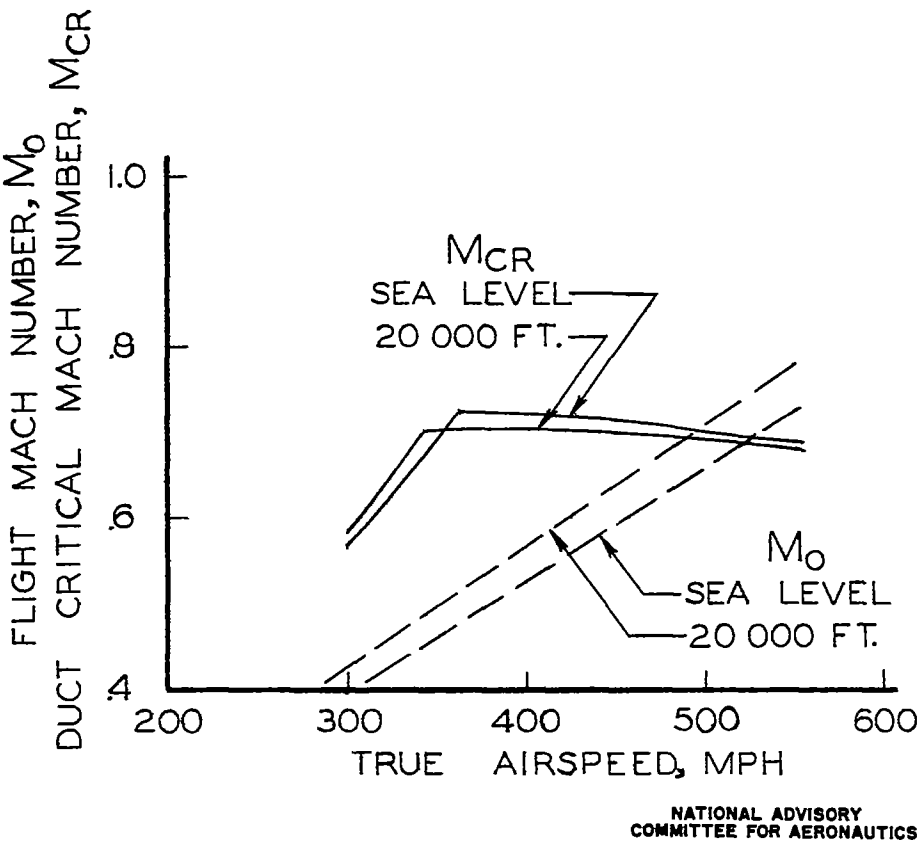

FIGURE 17.-VARIATION OF THE SUBMERGED-DUCT-ENTRY ESTIMATED CRITICAL MACH NUMBER WITH TRUE AIRSPEED FOR THE FIGHTER AIRPLANE. "MATCHED" FLIGHT CONDITIONS AT SEA LEVEL AND 20,000 FT.

CONFIDENTIAL